

# A DOUBLE-POROSITY POROELASTIC MODEL TO RELATE P-WAVE ATTENUATION TO FLUID FLOW IN VUGGY CARBONATE ROCK

Jorge Parra<sup>1</sup> and Chris Hackert,<sup>1</sup> Steven Pride<sup>2</sup>

<sup>1</sup>) Southwest Research Institute, San Antonio, Texas, USA

<sup>2</sup>) Geosciences Rennes, University de Rennes 1, Rennes Cedex, FRANCE

**Abstract:** A pressure source in a fluid-filled porous formation (a South Florida aquifer) excites P waves that compress the pore volume. This results in increasing pore pressure, which induces fluid flow in the carbonate rock. Fluid flow is modeled by assuming that the correlation length based on the heterogeneous pore structure corresponds to a double porosity medium. We determine pore structure using computer tomography. We also use well logs to estimate fluid and poroelastic properties, and we construct a double-porosity model to predict attenuation and spectral fluid pressure responses in the frequency range of 0.01-100 kHz. We find that the high fluid pressure is controlled by permeability, and the wave motion can excite slow waves observed as oscillations in the low frequency part of the spectrum. The results demonstrate how rapidly the slow waves vanish in low permeability regions, and that the fluid pressure drop is greater for fluid transport between the large vugs and the matrix.

## 1. INTRODUCTION

When compressional, or P, waves excited by a seismic source propagate in an aquifer that is characterized by heterogeneities of different dimensions, such as variations in lithology and vuggy porosity, different regions respond with different fluid pressures. The associated fluid-pressure diffusion attenuates the wave energy. Three types of waves can be identified – a fast and a slow P wave and a shear wave. For the fast P wave, the pore fluid and porous matrix are compressed simultaneously; for the slow P wave, the porous matrix relaxes when the pore fluid is compressed.

In general, in a homogeneous fluid-filled porous medium, when the passing wave induces small fluid pressure gradients between regions of compression and extension, these gradients cause fluid flow relative to the solid. The fluid flow incurs viscous loss, resulting in a small attenuation of the passing wave. However, in real rocks this phenomenon is overwhelmed by local flow effects such those observed by Mavko and Nur (1975). These effects are caused by the pore fluid between regions of different compliances under the compression (or extension) induced by the passing wave. In an application given by Gurevich et al. (1997) for a medium composed by thin alternating layers of two poroelastic materials with different compliances, propagation of a P-wave will squeeze the fluid from more compliant into the less compliant layers. This local flow of the pore fluid is accompanied by the viscous loss and results in the attenuation of the passing wave. On the other hand,

in an aquifer when the P-waves compress an element containing mesoscopic heterogeneity, the different porosity types should respond with different changes in their fluid pressure. An internal equilibrium then takes place with fluid flowing from the more compliant high-pressure regions to the relatively stiff low-pressure regions. Such mesoscopic flow attenuates energy and affects the wave amplitude.

In this paper we investigate the attenuation and fluid pressure due to mesoscopic flow in a double-porosity medium. The medium we analyze is an aquifer characterized by pore structure formed by a matrix and vuggy porosity. Attenuation curves of double porosity models are calculated using the theory developed by Pride and Berryman (2003). The Green function for a volume source in a double porosity effective medium is developed for calculating fluid pressure spectral responses and seismic signatures based on typical vuggy carbonate rock properties from South Florida.

## 2. PROBLEM FORMULATION

To calculate the pore pressure response due to a volume source we use the Green's function based on the effective Biot theory. We write the coupled system of equations directly from the constitutive relations given by Biot (1962). These are the total stress of the isotropic porous medium, the stress in the porous fluid, the momentum balance equation for total stress, and the generalized Darcy's law. Following Parra (1991) and Boutin et al. (1987), the coupled system of differential equations in the

frequency domain for a volume source (V) and a force (F) is given by:

$$\mu \nabla^2 u + (\lambda + \mu) \nabla \nabla \cdot u + \omega^2 \bar{\rho} - \bar{\alpha} \nabla p = -F \quad (1a)$$

$$\theta \nabla^2 p - \beta p - \bar{\alpha} \nabla \cdot u = -V, \quad (1b)$$

where  $u$  is the particle vector displacement of the solid,  $p$  is the fluid pressure, and

$$\bar{\rho} = \rho + \rho_f \omega^2 \theta$$

$$\bar{\alpha} = \alpha + \rho_f \omega^2 \theta$$

$$\lambda = K_d - 2\mu/3$$

$$\theta = \frac{jk(\omega)}{\eta\omega}$$

where  $\rho$  is effective bulk density, and  $\mathcal{E}$  " and  $\mathcal{S}$  are effective constants related directly to the complex Biot constants  $H$ ,  $C$  and  $M$  by:

$$\beta = \frac{I}{M} \quad (2a)$$

$$\alpha = \frac{C}{M} \quad (2b)$$

$$\lambda + \mu = H - G - C^2 / M. \quad (2c)$$

We also have the effective shear modulus relation,  $\therefore = G$ , and the effective parameter,  $\theta$ , which includes the effective fluid inertia in the relative motion parameter,  $\tilde{\rho}$ , i.e.,

$$\theta = -\frac{I}{\omega^2 \tilde{\rho}}, \quad (3)$$

where  $\tilde{\rho} = -\eta/[j\omega k(\omega)]$ ,  $k(\omega)$  is the complex frequency-dependent dynamic permeability, and  $\eta$  is the fluid viscosity.

The effective complex Biot constants  $H$ ,  $C$ , and  $M$  are defined in terms of the effective drained modulus of the composite  $K_d$ , the effective undrained bulk-modulus  $K_u$ , and the effective Skempton's coefficient  $B$  as

$$H = K_u + 4G/3$$

$$C = BK_u \quad (4)$$

$$M = \frac{B^2}{1 - K_d / K_u} K_u$$

where the effective complex functions  $K_d$ ,  $K_u$ , and  $B$  are given for double porosity materials by Pride and Berryman (2002).

The next step is to find the Green's function from Eq. (1). Parra (1991) solved this equation and developed a solution for the pressure source (or volume) using the Sommerfeld integrals. The fluid pressure in the frequency domain is given by

$$p = \frac{V_o(\omega)}{4\pi\omega^2\bar{\rho}} \left[ \frac{\delta_1}{\alpha_3} \left( \frac{e^{j\lambda_1 R}}{R} \right) - \frac{\delta_2}{\alpha_3} \left( \frac{e^{j\lambda_2 R}}{R} \right) \right] \quad (5)$$

where  $R$  is the distance between the source and receiver, and the parameters  $\lambda_1, \lambda_2$  are the wave numbers associated with fast and slow P waves travelling in an effective porous medium. The first and second terms in Eq. (5) are the fast and slow P waves, respectively. Wave numbers that control the phase velocity and attenuation of the wave travelling in the effective porous medium are summarized as follows:

$$\lambda_1 = [(b + \Delta) / 2]^{1/2} \quad (6)$$

$$\lambda_2 = [(b - \Delta) / 2]^{1/2}$$

where  $b = k_p^2 - \bar{\alpha}^2 / (\lambda + 2\mu)\theta - \beta / \theta$

and  $\Delta = [b^2 + 4k_p^2\beta / \theta]^{1/2}$

in which  $k_p^2 = \omega^2 \bar{\rho} / (\lambda + 2\mu)$ .

In Eq. (5), the factors of the terms containing the exponentials are obtained from the relations given by

$$\delta_m = \frac{\lambda_m^2 - k_p^2}{2\theta(\lambda_1^2 - \lambda_2^2)};$$

for  $m = 1, 2$  and  $\alpha_3 = 1 / 2\bar{\rho}\omega^2$ .

### 3. RESULTS

We use cores and well logs to construct and verify a double porosity model. Core data provide images of pore structure, such as matrix porosity and range of vug dimensions and physical properties (Figure 1). Velocity, porosity and density logs provide poroelastic properties. Permeability is derived from NMR well logs. These data are given in Parra and Hackert (2002) and Parra et al. (2002). Based on the solution given by Pride and Berryman (2002), we assume a spherical vug of radius  $a$  surrounded by a homogeneous porous matrix.

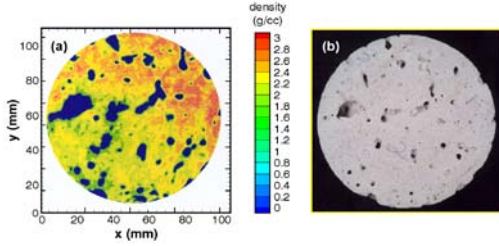


Figure 1. (a) Computed density from x-ray CT data, and (b) photograph of the end of the core.

The bulk modulus  $K_1$  of the rock matrix in terms of the grain density,  $\rho_s$ , the P- and S-wave velocities of the dry skeleton ( $v_p$ ,  $v_s$ ), and the porosity  $\phi_1$ , allow us to constrain the double porosity model by use of the well log data and the equation,

$$K_1 = (1 - \phi_1) \rho_s (v_p^2 - \frac{4}{3} v_s^2). \quad (7)$$

From this data, we determine the following fluid and carbonate properties to construct the model:

$$\begin{aligned} K_s &= 72.2GP & \eta &= 0.001P \bullet s \\ G_s &= 38.6GP & v_p &= 2276m/s \\ \rho_s &= 2650kg/m^3 & v_s &= 1036m/s \\ v_f &= 1500m/s & \phi_1 &= 35\% \\ \rho_s &= 1000m/s & \phi_2 &= 45\% \end{aligned}$$

Alternatively, to simulate the bulk modulus of the vuggy structure we consider that soft materials are embedded in the interconnected pore matrix containing vugs. In this case we use the relationship (Pride et al., 2002),

$$K_2 = K_s \frac{(1 - \phi_2)}{(1 + c\phi_2)}, \quad (8)$$

Where  $K_s$  is the modulus of the solid grain,  $\phi_2$  is porosity, and  $c$  is a consolidation parameter that represents the sediments and fluid inside the vugs (unconsolidated material). We use  $c = 200$ . The effective compressional modulus (harmonic average of the  $K_1$  and  $K_2$  drained moduli) and the shear bulk modulus,  $G$ , of the double porosity medium can be obtained, respectively, from

$$K = \frac{K_1 K_2}{d_2 K_1 + d_1 K_2}, \quad (9a)$$

$$G = (1 - \phi) \rho_s v_s^2, \quad (9b)$$

Where  $\phi$  is the effective porosity of the double porosity medium given by

$$\phi = \phi_1 d_1 + \phi_2 d_2. \quad (10)$$

The values of  $d_1 = 0.963$  and  $d_2 = 0.037$  are for a little sphere embedded in a stiff porous matrix with interconnected pore structure, as given in Pride and Berryman (2003).

Vug size varies in the pore matrix, with typical lengths from 1-6 cm. In the core in Figure 1, vugs are 15-20 mm in length. Based on NMR logs, we find that permeability in the region of interest varies from 1-4 Darcies. Using these data we produce attenuation curves for vugs of dimensions  $a = 1, 1.5, 2$  and  $3$  cm, in an effective medium having a permeability of 3 Darcies, as shown in Figure 2a. In this case the fluid flows easily from pore matrix to vugs and vice versa. Attenuation peaks are shifted to low frequency range as vug dimension increases. The mesoscopic heterogeneity (vug) of characteristic length  $L = 1.92a$  equilibrates the pressure at a frequency

$$f = D/L^2 \quad (11)$$

where  $D$  is the pore-pressure diffusivity given by

$$D = \frac{k BK}{\eta \alpha} \quad (12)$$

and where  $k$  is permeability,  $B$  is Skempton's coefficient,  $K$  is drained bulk modulus, and  $\alpha$  is the Biot-Willis coefficient of the medium. For given fluid and rock physical properties, frequency is inversely proportional to the characteristic length,

L. This makes attenuation peaks shift downward with increasing vug size. The calculated equilibrium frequencies ( $f_{meso}$ ) for heterogeneities with radii of 1.0 cm, 1.5 cm, 2.0 cm, and 3.0 cm are 4446 Hz, 1976 Hz, 1112 Hz, and 494 Hz, respectively.

To relate attenuation to fluid dynamics, we calculate the fluid pressure response due to a pressure source (or volume source) located 100 m from a pressure detector. The pressure response is calculated in MPa as a function of frequency, as shown in Figure 2b, for  $a = 1$  to 3 cm. Each curve shows an increase in pressure to a maximum and then a sharp decrease to a minimum to values near the mesoscopic frequency ( $f_{meso}$ ). The plots show that as vug dimension increases pore pressure decreases in the frequency range of 3-1000 Hz. The pressure peaks are shifted to the lower frequencies as vug size increases. An internal equilibrium takes place as the pulse deforms the pore space, and fluid will tend to flow from compliant high-pressure regions to relatively stiff low-pressure regions (less compliant regions). Such mesoscopic flow reduces wave amplitude. In fact, the maximum pressure for each correlation length (vug dimension) occurs at a frequency less than the corresponding mesoscopic frequency and at lower attenuations. Lower frequency corresponds to long periods for a travelling pressure pulse. Long periods (low frequencies) provide sufficient time for the flow to occur during one-half period of the wave cycle. Thus, the fluid pressure will equilibrate and the rock will be in a relaxed state.

At high frequencies (short periods) there is not enough time for flow to occur, and the rock is in an unrelaxed state, thus, the rock is stiffer at high frequencies and has higher wave velocities. At intermediate frequencies, interactions between fluid and solid is at a maximum, and a maximum attenuation occurs. In this case, the wave amplitude is reduced practically to zero.

In Figure 2b we observe that in the frequency range between 3-750 Hz, the spectra exhibit rapid oscillations. This part of the spectra captures the slow P-wave motion due to propagation of a pulse in the fluid (water) of the aquifer when the matrix is relaxed (or in state of equilibrium). Oscillations in the spectrum arise from phase differences in the slow and fast waves. As seen in Figure 2b, these rapid oscillations occur for each of the pressure peaks. This suggests that the slow wave can be excited at frequencies equal to or less than the mesoscopic frequency.

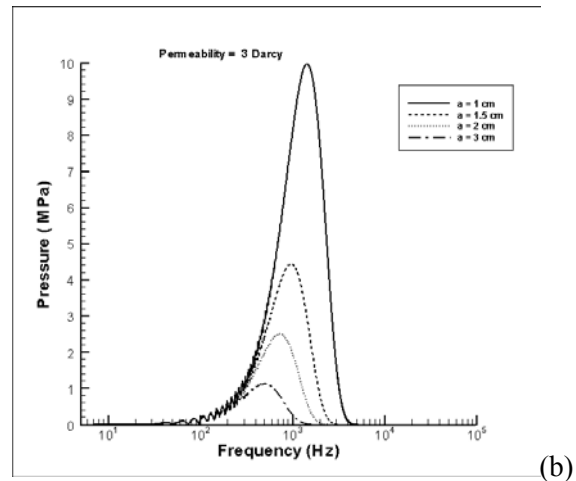
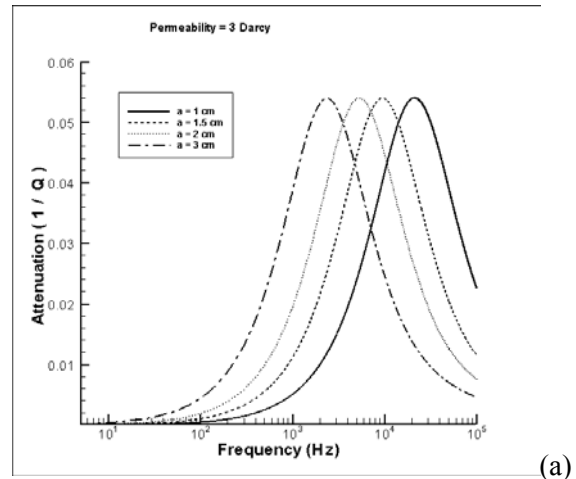


Figure 2. (a) Attenuation curves and (b) pressure spectral response illustrating the length scale effect on attenuation and fluid pressure.

To analyze this effect in more detail, we calculate the spectrum of slow P waves only by using the second term of Eq. (5). Figure 3 shows the spectra of slow P waves for  $a = 1-3$  cm. The curves show pressure sensitivity to vugs in the pore matrix; the fluid pressure is sensitive to vugs at frequencies greater than 100 Hz. For frequencies less than approximately 100 Hz, the fluid pressure amplitude should remain unchanged.

The high permeability of the carbonate aquifer (easy flow) provides the right conditions for part of the P-wave energy to compress the fluid and excite slow waves. This phenomenon can also be seen in the time domain. A pressure source having a peak source frequency of 300 Hz excites fast and slow P waves that are recorded by a pressure detector at a horizontal distance of 100 m. The waveforms are calculated for  $a = 1, 1.5, 2,$  and 3 cm vugs, in an

effective medium of permeability = 3 Darcies (see Figure 4). In the traces, the fast P wave arrives with a velocity of 2450 m/s, which agrees with the P-wave velocity log. The second event observed in each trace is the slow P wave that travels with a velocity of 1250 m/s. As expected when vug size increases, the amplitude of the fast P wave is more attenuated, and the amplitude of the slow P wave remains approximately the same. It is not affected by vug size as long as permeability does not vary.

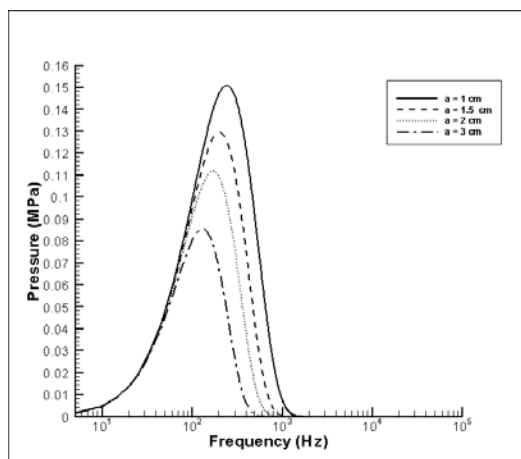


Figure 3. Slow-wave pressure spectral responses illustrate the length scale effect on fluid pressure.

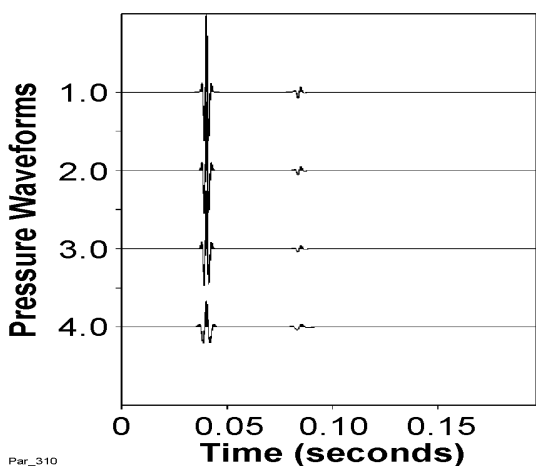


Figure 4. Pressure waveforms illustrating the length scale effect on fast and slow P-wave events. Waveforms correspond to vug sizes of 1, 1.5, 2, and 3 cm, in a matrix of 3 Darcy permeability.

In the second example given in Figure 5, we examine how permeability affects interconnected vugs. We assume that fluid will flow from the vugs to the pore matrix with the same permeability for a

given length scale. We vary permeability from 1-3 Darcies for a vug size of 2 cm. As in the previous example, the mesoscopic heterogeneity has a characteristic length ( $a = 2$  cm), and the fluid pressure equilibrates when the frequency is  $f = D/L^2$ . According to Eq. (12), pore pressure diffusivity  $D$  is proportional to permeability, which causes the mesoscopic attenuation peaks to shift upward to higher frequency with increasing permeability for a given heterogeneous medium, as shown in Figure 5a. For low frequencies, fluid pressure will attenuate more as permeability decreases (Figure 5b). This means that at lower frequency (long periods), fluid motion (from vugs to pore matrix) becomes unrelaxed in low permeability environments, and the presence of slow waves is diminished (i.e., less fluid pressure decreases the generation of slow waves). In a more permeable medium (e.g., 3 Darcies), fluid pressure increases and the slow wave can be excited and will be less attenuated.

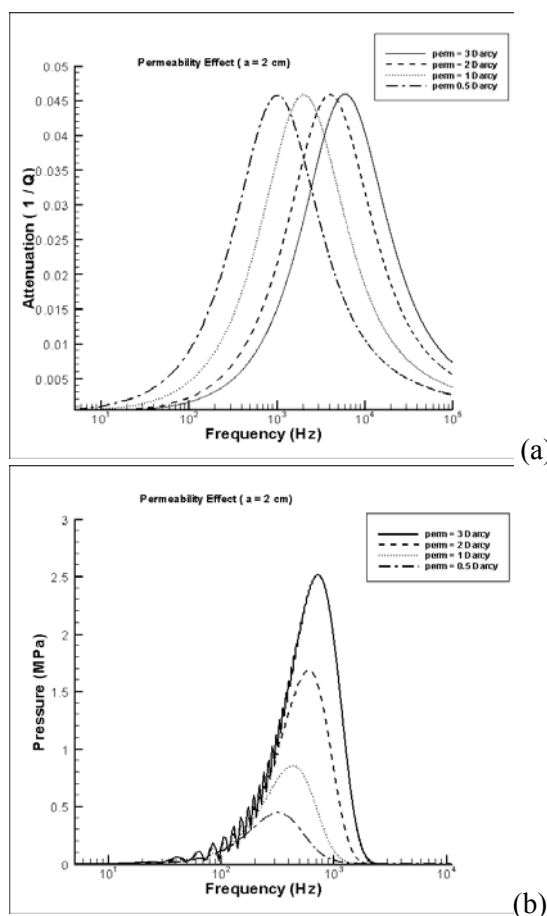


Figure 5. (a) Attenuation curves and (b) pressure spectral response illustrate the effect of permeability effects on fluid pressure attenuation.

Finally, we calculate synthetic seismograms for this model to show the effect of fast and slow P waves as a function of permeability. Each trace of Figure 6 represents different permeability. The waveforms were produced for a peak source frequency of 300 Hz. At this frequency, both waves are sensitive to permeability. For frequencies  $\leq 100$  Hz (see Figure 5), as permeability decreases, the amplitude of the fast P wave remains about the same, but slow wave amplitude decreases as permeability decreases.

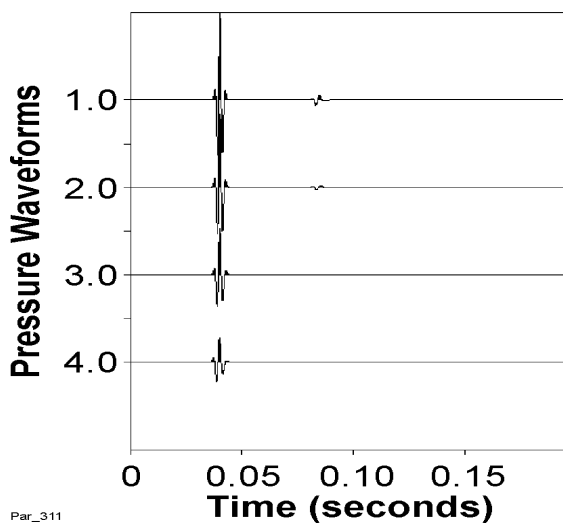


Figure 6. Pressure waveforms illustrating permeability effects on fast and slow P-wave events. Waveforms are for 0.5, 1, 2, and 3 Darcy permeability, with a vug of radius  $a=2$  cm.

#### 4. CONCLUSIONS

The effective double-porosity model was successfully adapted to the dynamic poroelastic wave equation to simulate P-wave and slow wave attenuation and spectral responses due to poroelastic fluid flow in vuggy carbonate rocks. We demonstrated that P-wave attenuation is sensitive to the pore structure of the carbonate rock formation. We found that the slow wave has a characteristic spectral signature that can be detected with seismic techniques in formations having interconnected vuggy porosity. This suggests that the hydraulic properties of vuggy zones can be inferred from P-wave attenuation measurements. The present solution allows us to relate the amplitude of fluid pressure oscillations to the attenuation of the wave motion, thus enhancing our understanding of coupling between the poroelastic fluid-flow and the

vuggy porous matrix when conducting monitoring surveys.

#### ACKNOWLEDGMENTS

Program work was supported by contract DE-FC26-02NT15343 from the U.S. Department of Energy, National Petroleum Technology Office. The assistance of P. Halder (DOE) is gratefully acknowledged.

#### REFERENCES

- Biot, M.A., 1962. *Mechanics of deformation and acoustic propagation in porous media*, Journal of Applied Physics 33: pp. 1482-1498.
- Boutin, C., Bonnet, G., and Bayard, P.Y., 1987. *Green functions and associated sources in infinite and stratified poroelastic media*, Geophysical Journal Astronomic Society 90: pp. 521-550.
- Gurevich, B., Zyryanov, V.B., and Lopatnikov, S., 1997. *Seismic attenuation in finely layered porous rocks: Effects of fluid flow and scattering*, Geophysics 62: pp. 319-324.
- Mavko, G., and Nur, A., 1975. *Melt squirt in aethenosphere*, Journal Geophysical Research 80: pp. 1444-1448.
- Parra, J.O., Hackert, C.L., Collier, H., and Bennett, M., 2001. *A methodology to integrate magnetic resonance and acoustic measurements for reservoir characterization*, Report DOE/BC/15203-3, National Petroleum Technology Office, Department of Energy, Tulsa, OK. ([www.reservoirgeophysics.swri.edu](http://www.reservoirgeophysics.swri.edu)).
- Parra, J.O., 1991. *Analysis of elastic wave propagation in stratified fluid-filled porous media for interwell systemic applications*, Journal of the Acoustic Society of America 90: pp. 2557-2575.
- Parra, J.O., and Hackert, C.L. 2002. *Wave attenuation attributes as flow unit indicators*, The Leading Edge, June 2002: pp. 564-572.
- Pride, S., Tromeur, E., and Berryman, J., 2002, *Biot slow-wave effects in stratified rocks*, Geophysics 67: pp. 271-281.
- Pride, S., and Berryman, J., 2002. *Attenuation of P waves by wave-induced fluid flow*, Proceedings of the second Biot Conference on Poromechanics, Auriault et al. (eds.), Grenoble, France, pp. 739-744.
- Pride, S., and Berryman, J., 2003. *Linear dynamics of double-porosity and dual-permeability materials*, submitted to Geophysical Letters.

